

Simulation study of axial ultrasound propagation in heterogeneous cortical bone model

不均一な皮質骨モデルにおける骨軸方向の
超音波伝搬シミュレーション

Koki Takano^{1†}, Yoshiaki Nagatani² and Mami Matsukawa¹
(¹Doshisha Univ.; ²Kobe City Coll. Tec.)

高野幸樹^{1†}, 長谷芳樹², 松川真美¹(¹同志社大, ²神戸高専)

1. Introduction

Osteoporosis is a skeletal disease that reduces bone mineral density (BMD) and increases the risk of fracture. Early detection and rapid care are both necessary for prevention of fractures. The current standard for the evaluation of osteoporosis is dual-energy X-ray absorptiometry (DEXA). However, this method is not suitable for mass screening because it requires the presence of specialists, and involves X-ray radiation exposure. Quantitative ultrasound (QUS) is therefore commonly used because it enables the measurement without the problems of DEXA. One of the QUS method, Axial Transmission (AT) technique, offers the potential to estimate both the mineral density and the elastic properties of cortical bone. Because the cortical bone supports the body load, fractures of this bone directly decreases the quality of life. The AT technique currently measures the first arriving signal (FAS) which is a leaky wave from the bone surface. Talmant et al. has reported that the FAS velocity relates to age [1]. However, most of FAS simulation studies assume that bone is uniform, which does not reflect the actual anisotropic and heterogeneous character of bone [2].

In this study, using an experimental data of actual cortical bone, we constructed a three-dimensional (3D) model of bone with anisotropic and heterogeneous elasticity, and studied the ultrasonic wave propagation in the model using a FDTD simulation.

2. Samples

The samples used in the velocity distribution measurements were obtained from a 73-month-old female bovine. We sliced the long bone of bovine tibia into 4 samples with thickness of 10 mm. Two fine holes were additionally drilled in each sample to act as position markers before they were sliced. The simulation area in one sample is shown in **Fig. 1**.

3. Experimental method

Figure 2 shows the experimental setup used. One cycle of sinusoidal wave at frequency of 1 MHz

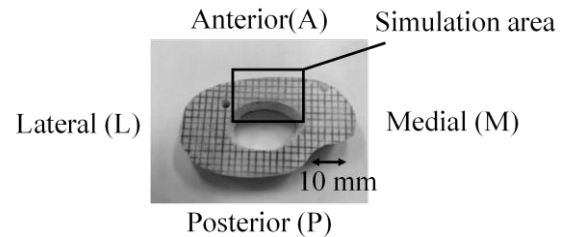


Fig. 1 Bovine cortical bone samples.

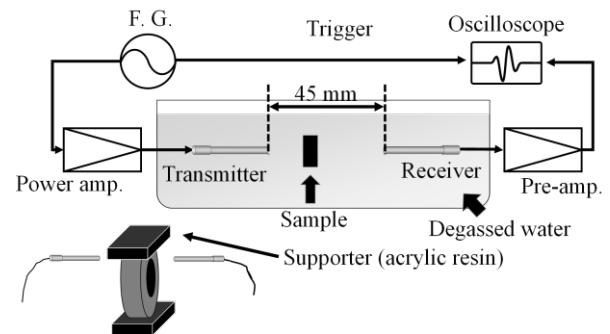


Fig. 2 Experimental setup used.

with amplitude of 5 V_{p-p} was delivered from a function generator (Agilent Technologies, 33250A). Then, after amplified 20 dB using a power amplifier (NF, HSA 4101), the signal was sent to a flat transmitter made from polyvinylidene fluoride (handmade, 3 mm diameter). The ultrasonic waves that passed through the sample were measured at the receiver (handmade, 3 mm diameter) and recorded in a digital oscilloscope (Tektronix, TDS 524A) after a 20 dB amplification (NF, BX-31). The transmitter was set 45 mm apart from the receiver. The samples were held between them using acrylic plates, and here the bone axis was set equal to the direction of wave propagation. The sample position was changed to measure the distribution of the longitudinal wave velocities with the spatial resolution of 1 mm. The bone thickness at each measurement point was precisely measured using a micrometer.

The wave velocity in a bone sample was calculated from the arrival time difference between waves passed through only water, or bone and water. The velocities in the outer part were lower than those in the inside part.

4. Simulation method

In this study, a 3D elastic finite-difference time-domain (FDTD) method was used [3]. The simulation area was the anterior part of the bone. The bilinear interpolation and the PCHIP (Piecewise Cubic Hermite Interpolating Polynomial) were used for a 3D FDTD model fabrication [4]. We assumed that the bone had uniaxial anisotropy to estimate elastic constants. To estimate all constants in all positions, we assumed that the Poisson ratio was 0.33 [5] and referred to studies by Nakatsuji and Yamato for anisotropy information of bovine cortical bone [6,7]. In the model, the outside elastic constants under receivers were mostly low reflecting the distribution of velocity. **Fig. 3** shows (a) the simulation condition and (b) cross section view of the model used in this study. The left side of the model was expanded by 16 mm to avoid wave reflection. The Higdon's second-order absorbing boundary condition was applied to the boundary of the simulation area. In the simulation, the spatial resolution was 40 μm and the time resolution was 4.6 ns. The input signal was a single sinusoidal wave with a frequency of 1 MHz with a Hanning window.

5. Result and discussion

We have decreased the thickness from the under (inner) part of the bone, simulating the osteoporotic bones. The thicknesses of the models were A) 6.5 mm, B) 4.7 mm, C) 3.7 mm, D) 2.7mm, and E) 1.7 mm. **Fig. 4** shows the sound fields of model A and model E. The FAS wave velocities were calculated from the arrival time difference. **Fig. 5** shows the FAS wave velocities obtained by the simulation using the heterogeneous model. Wave velocities in all models decreased. Because the FAS mainly propagates on the surface of bone, it seems to depend on the changes of surface elastic constants. In the model E, velocities were smaller than those in other models. This is because the velocities of the inside part (high velocity part) was removed. Although the AT technique measures surface FAS velocity, it gradually reflects elastic properties of inner part during propagation. In addition, the effect of removal gradually increases as the propagation distance becomes longer. As a result, FAS was gradually affected by the inner part as the wave propagates.

6. Conclusion

In this study, we focused on the effect of thickness of heterogeneous and anisotropic cortical bone during the axial transmission of ultrasonic wave. The FAS velocities changed as the propagation distance becomes longer. This is because elastic constants of inner part affect the FAS velocity. Therefore the FAS velocity in heterogeneous and anisotropic bone may include

information of elastic properties of both surface and inner parts.

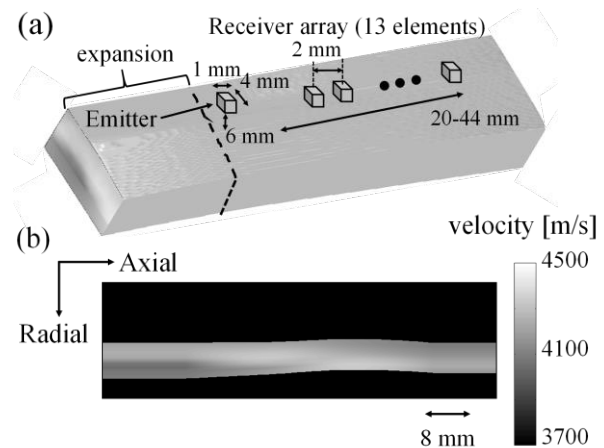


Fig. 3 FDTD Simulation model.

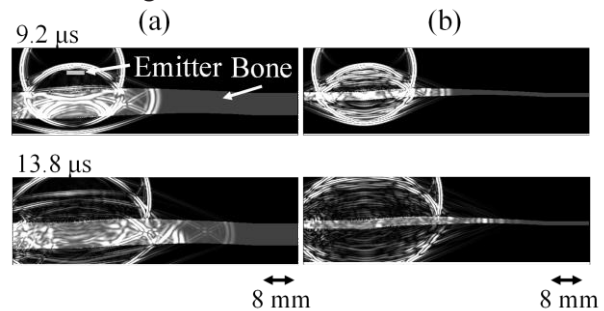


Fig. 4 Sound fields of (a) model A, and (b) E.

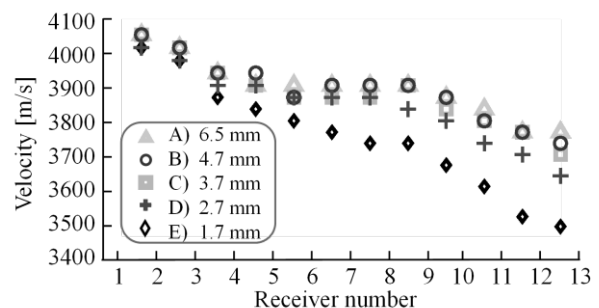


Fig. 5 FAS wave velocities between receivers.

Reference

1. M. Talmant, et al., *Ultrasound Med Biol*, **35**, pp. 912-919 (2009).
2. Y. Yamato, et al., *IEEE, TUFFC*, **55**, pp. 1298-1303 (2008).
3. Y. Nagatani, et al., *Jpn. J. Appl. Phys.*, **45**, 7186 (2006).
4. F. N. Fritsch, et al., *SIAM J. Numerical Analysis*, **17**, pp.238-246 (1980).
5. T. H. Smit et al., *Journal of Biomechanics*, **35**, Issue 6, pp. 829-835 (2002).
6. T. Nakatsuji, et al., *Jpn. J. Appl. Phys.*, **50**, 07HF18 (2011).
7. Y. Yamato, et al., *Calcif Tissue Int.*, **82**, pp. 162-169 (2008).